Available online at www.sciencedirect.com

ScienceDirect

Physics Procedia 67 (2015) 822 – 827

Physics Procedia

25th International Cryogenic Engineering Conference and the International Cryogenic Materials Conference in 2014, ICEC 25–ICMC 2014

On the mystery of using helium's second sound for quench detection of a superconducting cavity

R. Eichhorn[a,*] and S. Markham[a]

[a]*Cornell Laboratory for Accelerator-based Science and Education (CLASSE), Cornell University, 161 Synchrotron Drive, Ithaca, NY 14853 USA*

Abstract

The detection of a second sound wave, excited by a quench, has become a valuable tool in diagnosing hot spots and performance limitations of superconducting cavities. Several years ago, Cornell developed a convenient detector (OSTs) for these waves that nowadays are used world-wide. In a usual set-up, many OSTs surround the cavity and the quench location is determined by triangulation of the different OST signals. Convenient as the method is there is a small remaining mystery: taking the well-known velocity of the second sound wave, the quench seems to come from a place slightly beyond the cavity's outer surface. We will present a model that might help explaining the discrepancy.

Peer-review under responsibility of the organizing committee of ICEC 25-ICMC 2014

Keywords: second sound; superconducting RF; quench detection

1. Introduction

Many future linear accelerators rely on superconducting radio frequency (SRF) cavities to accelerate the particles. During the last decade, the advantages of SRF technology compared to normal conducting RF systems based on copper resonators have been broadly recognized. Early SRF cavities (in the 1980's) had low accelerating gradients, rather high RF losses and, being the most serious issue, a very unreliable performance reproducibility. Today, SRF cavities have overcome these limitations: they reach high gradients and low losses, very close to the theoretical limit, and the performance has improved dramatically. Many of the advances in the field are due to a better understanding of the surface effects in SRF cavities, quench limits and contamination.

* Corresponding author. Tel.: +1-607-255-2328; fax: +1-607-254-4552
E-mail address: r.eichhorn@cornell.edu

Peer-review under responsibility of the organizing committee of ICEC 25-ICMC 2014
doi:10.1016/j.phpro.2015.06.138

A quench is often the limiting factor to a cavity's performance. Quenches are generally thought to be caused by defects on the inner surface of the cavity, which succumb to ohmic heating much more rapidly than the surrounding area of the cavity. Locating quench spots has been a major key in understanding SRF cavity performance. This can be done by locating temperature maps around the cavity (with typically more than 1000 sensors) or, in a more modern way, (see Padamsee (2008)) by using Oscillating Superleak Second Sound Transducers (originally developed by D. Hartill in Cornell, Conway (2009), as several research groups have been doing in recent years (e.g. Maximenko (2010)). The method is based on the 2nd sound waves in superfluid helium propagating outward from any heated area of a resonator. By testing a superconducting resonator in a superfluid helium bath it is possible to observe the second-sound temperature and entropy waves driven by the conversion of stored RF energy to thermal energy at a defect. By measuring the time of arrival of the 2nd sound wave-front at the detectors relative to the time of the resonator field collapse the distance between each transducer and the defect heated region may be calculated. This information is used to triangulate the defect location using the well-known temperature dependent propagation velocity of the sound wave. A common problem in this triangulation is that the source of the second sound wave seems to be located above the cavity surface, giving rise to various theories as the propagation speed of the wave seems to be greater than the published data. Most commonly, a sphere of uncertainty, usually 5 mm in radius has been assumed and a surface point, closest to the triangulated 2nd sound source location has been considered as quench location. Previous reports on computational approaches have verified the hypothesis that the radius of the defect increases to centimeters in size within a couple of milliseconds, which Antipov (2011) accounts for the discrepancy. We hypothesize that there may be an additional distance error due to a second sound wave being triggered a fraction of a millisecond before there is a noticeable loss in stored energy of the cavity, which usually is taken to trigger a quench. We will show that this effect could contribute to the observed disparity.

2. Model specifications

A MATLAB computational model is used to investigate the time dependent dynamics of a superconducting radio-frequency (SRF) cavity with a known defect under medium field conditions. We were particularly interested in the potential disparity between the time of the triggering of a second sound wave on the Nb-HeII interface and the time where losses in stored energy of the SRF system become significant. In order to do so we allowed our model to have two free parameters: one being the heat flux level at which significant and detectable amplitude of the second sound wave is generated and the other being the drop in RF power at which a quench is realized. We will discuss our choice of parameters below and allow the readers to draw conclusions using different values for these parameters. Our model considers a niobium cavity with a surface defect which is characterized by normal conducting resistivity. The remainder of the cavity is initially in the superconducting state, and undergoes thermal breakdown. The basic mechanics of the simulation assumes a cylindrically symmetrical geometry, centered around the defect. This reduces the problem to a quasi two-dimensional problem. The basic methodology has been used before by Padamsee (2008) and Antipov (2011) for these sorts of models. The specifics of our model are based on canonical computational methods for heat conduction as published by Bloomberg (1996).

2.1. Discretization

The model separates a cylindrical disk of niobium into mesh elements, each with a different temperature, which results in different physical properties. The model then iteratively computes heat transfer and ohmic heat dissipation into each of the relevant mesh elements. The choice of time step to ensure numerical stability is chosen according to canonical methods described by Eftring (1990). The stipulation on the time step is:

$$\Delta t < \frac{C_{ij} 2\pi r_i \Delta r \Delta z}{K_{i-1,j} + K_{i+1,j} + K_{i,j-1} + K_{i,j+1}} \forall i, j \tag{1}$$

where C_{ij} is the specific heat capacity at cell (i,j) and $K_{i-1,j}$ is the thermal conductance between cell (i, j) and cell (i − 1, j), etc. These were calculated like

$$K_{i,j-1} = \frac{2\pi r_i \Delta r}{\Delta z (\kappa_{i,j-1} + \kappa_{i,j})/2} \tag{2}$$

and

$$K_{i-1,j} = \Delta z \cdot \left(\frac{\ln(r_i / r_{i-0.5})}{2\pi\kappa_{i-1}} + \frac{\ln(r_i / r_{i+0.5})}{2\pi\kappa_i} \right)^{-1} , \quad (3)$$

where $\kappa_{i,j}$ is the temperature dependent thermal conductivity of cell (i,j) and Δr and Δz are the radial and lateral step sizes, respectively. In order to ensure the time step was less than this quantity, we calculated the quantity for each cell in the mesh, found the minimum and multiplied that value by some constant less than one.

2.2. Resistivity, heat generation and power dissipation

The resistivity of the non-defective superconducting portion of the cavity is characterized solely by residual resistance and BCS resistivity, while the resistivity of the defect is characterized by joule heating according to the skin effect equation:

$$R_n = \sqrt{\frac{\omega\mu_0}{2\sigma}} , \quad (4)$$

where ω is the frequency and σ is the bulk conductivity of the material. We used data from Antipov (2014) to make a parametric fit of the data for the normal conducting state, which are plotted in Fig. 1. The surface resistivity of the superconducting surface is given by:

$$R_s = R_0 + R_{BCS} , \quad (5)$$

where R_0 is a constant determined by the specifics of the cavity and the testing environment (usually in the order of 5 nΩ) and R_{BCS} is a temperature dependent resistance of a superconductor in an RF field according to the BCS theory which we defined according to previous analytic studies by Vines (2007). Explicitly, R_{BCS} is approximated as:

$$R_{BCS} = (2.78 \cdot 10^{-5}\Omega)\frac{\nu^2}{t}\ln\frac{148t}{\nu}\exp-\frac{1.81g(t)}{t} , \quad (6)$$

with the parameters (reduced temperature, normalized frequency and energy gap of the superconductor):

$$t = \frac{T}{T_c}; \nu = \frac{f}{2.86GHz}; g(t) = \sqrt{\cos\frac{\pi t^2}{2}} . \quad (7)$$

The authors are well aware of the fact that various modifications of this formula exist with slightly different parameters. However, the results we derived and report below do not rely on a specific expression for the BCS resistance.

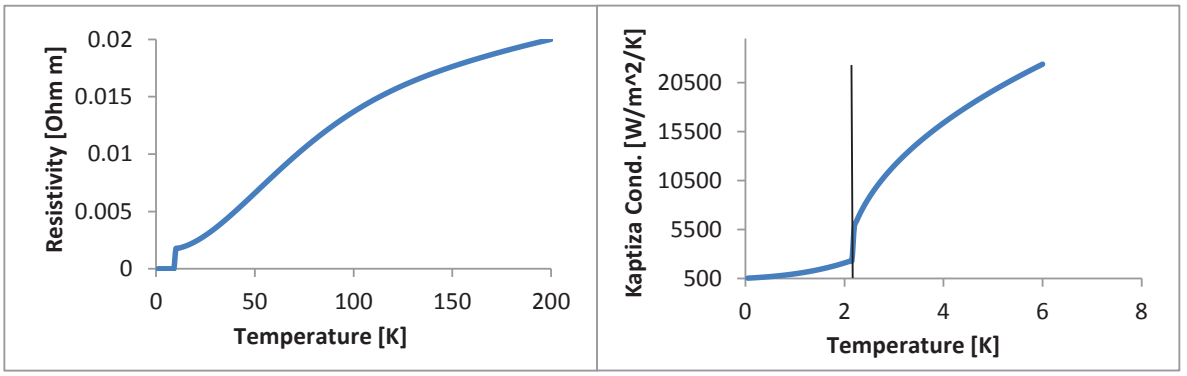

Fig. 1. Left: Resistivity of the niobium as a function of temperature, following a numerical fit by Vines (2007). Right: Kapitza conductance as a function of temperature. The vertical line indicates the lambda point of Helium.

The power dissipated due to ohmic heating is proportional to surface resistivity, governed by the following equation:

$$P_{diss} = \frac{1}{2} A R H^2, \tag{8}$$

where H is the magnetic field strength, R is the resistivity of the cavity surface in the area A, and A is the cross sectional area of the cavity.

2.3. Kapitza resistance

The Kapitza resistance at the niobium-helium II boundary is calculated using the following empirically fit equation by Mittag (1973) for un-annealed niobium in a bath of superfluid helium:

$$H_k(T_d, T_b) = 170 \frac{W}{m^2 K} \cdot \left(\frac{T_b}{1K}\right)^{3.62} \cdot \left(1 + \frac{3}{2}t + t^2 + \frac{1}{4}t^3\right) \text{ with } t = \frac{T_d - T_b}{T_b}. \tag{9}$$

Above the lambda point of helium, we used

$$H_k(T_d, T_b) = 1.2 \cdot 10^4 \left(\frac{T_d - T_b}{1K}\right)^{.45} \frac{W}{m^2 K}. \tag{10}$$

The full function is shown in Fig. 1. We performed several simulations accounting for the Kapitza resistance and several without. We found that the inclusion of Kapitza resistance changed the results by less than 1%, indicating that the Kapitza resistance is not a significant contributor to the thermal dynamics of an RF quench.

2.4. Cryogenic properties: heat capacity and thermal conductivity

Heat capacity and thermal conductivity of the Niobium were calculated according to empirical numerical fittings by Davis (2011) and Koechlin (1996). The fits are plotted in Fig. 2.

2.5. Geometry, material assumptions and free parameters

In our simulations, we investigated a small region of the disk at radius of 8 mm. We assumed the disk was niobium with a RRR value of 300 (which is typical for a SRF cavity material), cylindrically symmetrical, flat, and 2 mm in thickness. The helium bath temperature was set to be fixed at 2 K and we assumed an RF magnetic field strength of 1×10^5 A/m being reasonable for a cavity close to a quench.

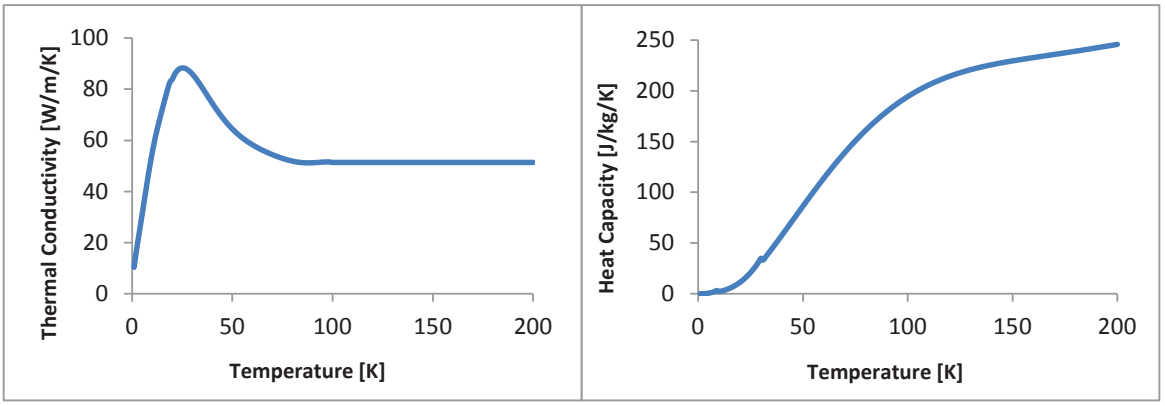

Fig. 2. Thermal conductivity (left) and heat capacity (right) of the Niobium used in our model. Data was taken from an analytical fit by Davies (2011) and Koechlin (1996).

We also made some assumptions about the nature of the second sound wave propagation. Theoretically, there exists no lower threshold for the entropy wave: the smallest change in temperature should be able to propagate through the helium. However, we found in a separate experiment (where the data analysis is still underway) that the detection of the second sound wave has an experimental lower limit. To make a conservative assumption, we chose that a second sound wave with detectable amplitude is triggered when the heat flux is greater than 1.5 W/cm^2. This choice was based on the heat flow through the helium becoming turbulent (theoretically described in 1930 by the Dittus-Boelter equation). It certainly represents a very high heat flux and more realistic values might be even an order of magnitude lower. How this would impact our conclusions will be discussed below.

3. Results

We ran our simulation, using the formulae given and the material parameters plotted above for the mesh size as specified. We used typical quench conditions, with a magnetic field strength of 0.126 T. The initial temperature of the niobium was set below the lambda point of helium at 2 K. A 0.2 mm defect was introduced at the center and we began the simulation in the normal conducting state. Starting with this initial condition we chose the time-step according to Eqn. (1) and recorded all relevant parameters. A visualization of the quench dynamics is shown in Fig. 3. We stopped the simulation when 2% of the cavity's stored energy had been dissipated in the quench, as we assumed that losses in the stored energy of the cavity to be significant and detectable. This assumption is based on a typical experimental set-up, where a cavity is driven by an RF system and a quench is detected by a change in the power balance.

We found that the noticeable loss in stored energy (according to our assumption made above) occurs 1.1×10^{-4} s after the initial quench conditions are set up. The second sound wave (under our conditions) is exited at 8.0×10^{-5} s. This already shows that there exist different time stamps for the quench for the different detection methods. With our assumptions we calculated that the second sound wave is excited 30 µs before the quench is noticeable on the RF side. This translates into a distance of more than 1 mm and explains why the second sound wave seems to come from a location above the surface: the second sound wave is generated before the quench is detected (but obviously after it occurred). These results can be seen in Fig. 4, allowing also to evaluate the effect of the choice of the free parameters: if you assume the second sound wave is excited at a heat flux level of 0.15 W/cm^2 (which the reader might find more reasonable) the time difference between the second sound wave excitation and the RF quench detection becomes 100 µs which then explains the spatial discrepancy of almost 5 mm, typically found in experiments. If one considers an RF detection limit of greater than 2% the time delay between the two incidents

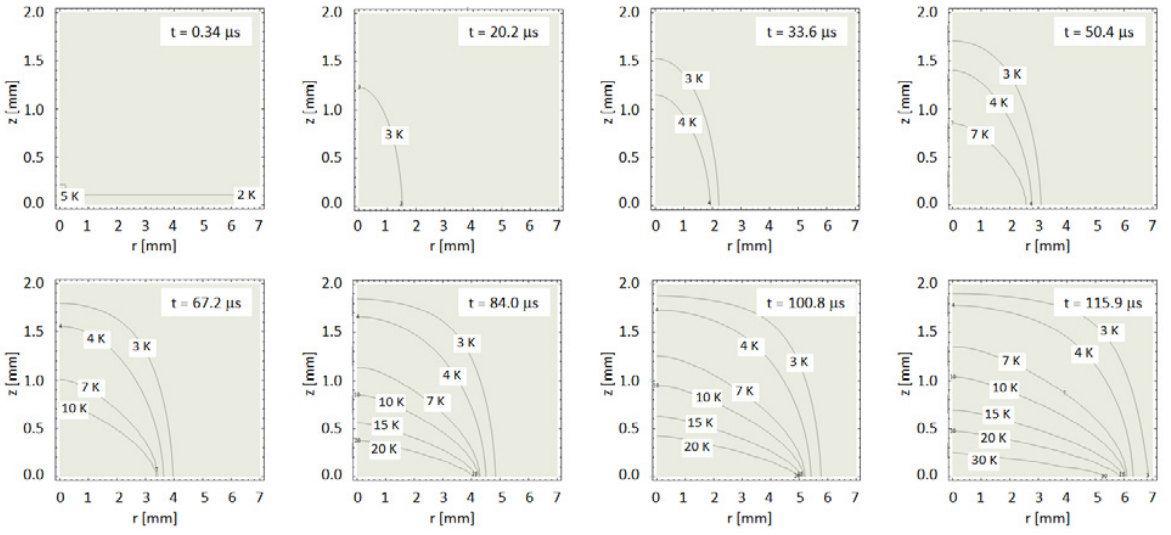

Fig. 3. Visualization of the quench spot and the heating as it expands in r and z direction. The heating spot is located in the lower left corner.

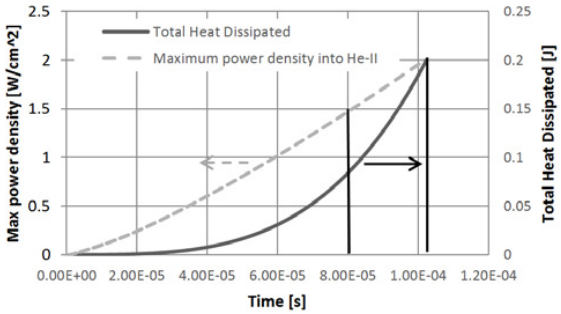

Fig. 4. Temporal evolution of two simulation outputs. The gap represents the delay between second sound wave trigger and quench detection.

increases and decreases when lowering the limit to 1% (which we think would be an extremely ambitious assumption). However, it should be noted that the dependency from that trigger level is less sensitive time-wise as the curve has a steeper slope.

4. Numerical stability

In order to test the validity of the model, we ran several simulations under identical conditions where the only altered feature was the mesh size. We calculated for radial steps ranging from 5 μm to 20 μm, and thickness steps in the same. We found that the results converged upon higher resolution. In particular, we found that the difference between the outputs of our highest resolution run and our second-highest resolution run was negligible. Thus, we chose our second-highest resolution model with a radial step size of 5×10^{-5} m and a z step size of 1×10^{-4} m.

5. Conclusion

Our calculations have revealed two potential sources for the systematic errors introduced when trying to localize quench inducing defects using OST second sound methods in quenched sc. cavities. We also found that the rate of power dissipation at the Nb-HeII interface reaches a level that would trigger a second sound wave potentially before a noticeable loss in the stored energy of the cavity occurs. If one defines the time of the quench as the moment the cavity energy noticeably decays and uses that to try to localize the quench inducing defect, this time may disagree with the time the second sound wave was actually produced by ≈ 30 μs. This would correspond to a systematic error on the order of 1 mm assuming the speed of second sound is about 20 m/s.

References

Padamsee, H., 2008, ."RF Superconductivity for Accelerators", Wiley Publications, Weinheim.
Conway, Z., et. al. 2009, "Defect Location in Superconducting Cavities Cooled with He-II Using Oscillating "Superleak 1 Proceedings of the International Conference on Superconducting Radio Frequency, Berlin.
Maximenko, Y. et. al., 2010, "Quench Dynamics in SRF Cavities: Can We Locate the Quench Origin with 2nd Sound?", Fermilab-Conf-11-152-TD.
Antipov, S. et. al., 2011, "2D Simulation of Quench Dynamics", Internal Report TD-11-017, Fermilab.
Bloomberg, T., 1996, "Heat Conduction in Two and Three Dimensions: Computer Modelling of Building Physics Applications". Lund University Publications.
Eftring, B., 1990, "Numerical calculations of thermal processes" (Written in Swedish) The Swedish Council for Building Research.
Antipov, S., 2014, " VTS Data parameterization" private communication .
Vines, J. et. al., 2007, "Systematic Trends for the Medium Field Q-Slope." Proceedings of the International Conference on Superconducting Radio Frequency, Peking Univ. Beijing, China.
Davies, A., 2011, "Material properties data for heat transfer modeling in Nb3Sn magnets", Illinois Accelerator Institute, pp. 17 – 18.
Mittag, K. , 1973, "Kapitza conductance and thermal conductivity of copper niobium and aluminium in the range from 1.3 to 2.1 K", Cryogenics 73, pp. 94–99.
Koechlin, E., Bonin, B., 1996, "Parametrization of the niobium thermal conductivity in the superconducting state", Superconducting Sci. Technol. 9.